Upstream and downstream influence of pipe curvature on the flow through a bend

John A. Fairbank and Ronald M. C. So*

Experiments were carried out to determine the upstream and downstream influence of a 180° pipe bend on the flow through the bend. A laser Doppler anemometer was used to measure the axial velocity at various locations before and after the bend. Two bends, of radius ratios 0.08 and 0.30, were studied at a Reynolds number of about 400, corresponding to Dean numbers of 110 and 220, respectively. Results indicate that the bend influence extended to one diameter upstream for a Dean number of 220, but no upstream influence was observed for a Dean number of 110. The corresponding downstream influence of the bend was 14 and 11 diameters, respectively. These results compare well to a recent analysis on entry flow into a pipe bend.

Keywords: *curved flows; curvature effects; upstream influence; downstream influence; pipe bends*

Introduction

Almost all piping systems contain bends. For example, the human cardiovascular system, heat exchangers, and ventilation systems all contain curved sections. In the human body, the aorta is strongly curved, as are many blood vessels. The study of flow through bends could contribute to the study of the cause of cholesterol buildup and the clogging of arteries, which would eventually lead to an understanding of heart attacks. In the case of heat exchangers, the development of secondary flows in bends alters the heat transfer characteristics of the system. Further, secondary flows can create points of maximum and minimum wall temperature and shear stress. A well-designed heat exchanger would require a sound understanding of the flow through the complicated piping system. Therefore, it is important to study the flow of fluids through curved pipes and bends to gain an understanding of the basic physics of these types of flows.

The study of curved flows began with the work of Dean,[1,2] who formulated the Dean number, De, as a measure of the pressure-induced secondary flow. Since De could be thought of as the ratio of the square root of the product of the inertia and centrifugal forces to the viscous force, it is a measure of the strength of the secondary flow. The Dean number is related to the Reynolds number and is equal to $(a/R)^{1/2}$Re. Therefore, for a given Reynolds number, the larger the Dean number, the stronger the secondary motion set up by the pipe bend. Since the pressure field in the bend gives rise to the secondary motion and thus sets up an adverse streamwise pressure gradient for the boundary layer on the outer wall at the bend inlet, and vice versa at the bend outlet, the presence of a bend in any piping system will affect both the upstream and downstream flow through the bend.

Numerous studies on curved flows have been carried out by various researchers since Dean's first investigation. A comprehensive review of these studies has been given by Berger *et al.*[3] These investigations included both laminar and turbulent flows with and without heat transfer through the pipe,[4–6] in pipe coils, [7,8] the developing and fully developed nature of curved flows,[9,10] circular as well as other cross-sectional geometries,[11] different entry flow conditions and their effects on the subsequent flow through the bend[12,13] and the relaminarization process in pipe coils.[14] Although these investigations covered a wide range of flow conditions and parameters, they were all concentrated on the flow in the curved section. Little was known of the upstream and downstream influence of pipe curvature on the flow through the bend. Among the studies on this last phenemenon, the work of Ito,[15] Rowe,[16] Enayet *et al.*,[17] Azzola and Humphrey,[6] and Yao and So[18] could be mentioned. Ito[15] measured the pressure drop for turbulent flow in a 90° bend and in the upstream and downstream tangents. His results provided quantitative information on the extent of the influence of the bend on the pressure gradient for a fully developed turbulent flow. Rowe[16] measured the cross-stream total pressure distributions inside a 180° bend and up to 61 pipe diameters downstream of the bend. Fully developed turbulent pipe flow, at a pipe Reynolds number of 2.36×10^5, was set up at the bend inlet. His results showed that bend curvature effects on total pressure distributions persist up to 30 diameters downstream of the bend. The work of Enayet *et al.*[17] was concerned with both laminar and turbulent flows through a 90° bend. Their studies showed a very slight upstream influence of bend curvature when the pipe Reynolds number was 500, and negligible influence when the Reynolds number was 1093 and higher. Downstream influence was very strong at one pipe diameter and was still quite noticeable at six pipe diameters for the turbulent flow case. Unfortunately, no measurements were made at six pipe diameters downstream of the bend for laminar flow through the bend, otherwise, some insight into the extent of downstream influence for laminar flow could be gleaned from their studies. Azzola and Humphrey[6] studied turbulent flow in a 180° bend and its downstream tangent for flow with Reynolds numbers of 57,400 and 110,000. However, they concentrated on the flow between $\theta = 177°$ in the bend and a location five diameters downstream of the bend. As a result, the true downstream influence of the bend on laminar flow through the bend was not known. On the other hand, Yao and So[18] used asymptotic expansion techniques and rapid distortion theory to analyze the flow in the entry region of a pipe bend and found that the upstream influence of pipe curvature was limited to a two diameter region.

Most of the laminar flow studies to date have dealt exclusively with the flow within a bend and have neglected the development of the flow in the upstream and downstream tangents. Of those studies dealing with curved circular pipes, most have dealt only with the entry condition of uniform velocity profile with different wall boundary layer thickness. Our aim was to attempt to fill some of this void by concentrating on laminar pipe flow

* Mechanical and Aerospace Engineering Department, Arizona State University, Tempe, AZ 85287, USA
Received 23 January 1986 and accepted for publication 1 December 1986

0142-727X/87/030211-06$3.00

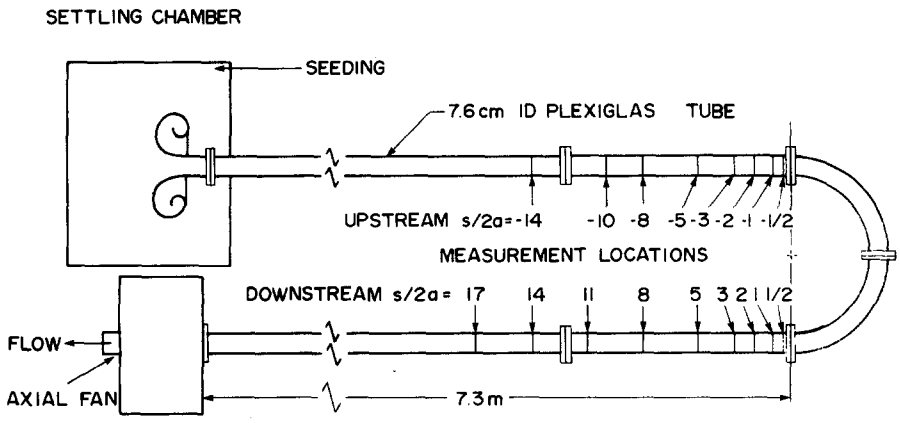

Figure 1 Schematic diagram of test rig and measurement stations

with the entry condition of fully developed flow and by emphasizing the flow before and after the bend. Therefore, measurements were taken in the upstream and downstream tangents of two 180° bends using laser anemometry to determine the extent and nature of the influence of the bend on both the upstream and downstream flow.

Experimental set-up

The experimental rig consisted of two straight Plexiglas pipes connected by a 180° bend (Figure 1). The straight sections were about 7.3 m long, or 96 diameters, to ensure fully developed flow at the entrance to the bend and at the exit of the rig. Air flow through the pipe was provided by a small axial fan located at the exit of the rig and separated from the circular pipe by a settling chamber with an area ratio to the tube of 30:1. The speed of the fan, and therefore the flow rate in the rig, was controlled by a Powerstat voltage regulator to keep the flow rate relatively constant. Over all the experimental runs, the rotormeter-measured flow rate varied by about 12%, whereas within any particular run, the flow rate varied by only about 2–3%.

At the entrance to the tube was a bell-shaped inlet and honeycomb flow straightener. Air was drawn out of a large settling chamber (cross-sectional area ratio to the tube of 80:1) to reduce the effects on the flow resulting from air motion in the room from the ventilation system. Seeding of the flow for the laser measurements was accomplished by depositing droplets of glycerine–water solution, of mean size about 1 μm, into the settling chamber instead of the tube itself to reduce disturbances to the flow created by the seeding.

Two bends were used in the experiment, with $\alpha = 0.30$ and 0.08, respectively. The $\alpha = 0.08$ bend was obtained by connecting two 90° PVC bends, which were obtained from PVC piping manufacturers. Even though these bends did not have an internal finish as smooth as the straight Plexiglas tube, and the pipe radius varied by as much as 1 mm, the flow through the bend was found to be unaffected. Flanges were attached to the ends of the 90° bends so that they could be smoothly connected to the straight tubes and to each other (Figure 1). The $\alpha = 0.30$ bend was formed by machining two half sections out of Plexiglas and joining them at the plane of symmetry. This method of bend formation ensured a perfect circular cross section in the $\alpha = 0.30$ bend. In all cases, the bend was oriented with its plane of symmetry horizontal. Axial velocity measurements were taken in both the upstream and downstream tangents of the pipe in three different planes: along the horizontal midplane of the tube ($y/a = 0$) and ± 17.8 mm away from the midplane ($y/a = \pm 0.46$). These data were used to construct isovelocity contours of the flow upstream and downstream of the bend and to illustrate the effect of bend curvature on the flow.

The velocity measurements were taken with a DISA model 55L laser Doppler anemometer (LDA) employed in the backscatter mode. The laser beam was split in two, and one of the two resultant beams was shifted in frequency by 40 MHz using a Bragg cell to allow the detection of negative velocities for the U velocity measurement. The beam intersection angle was 12.5°, yielding an ellipsoidal sampling volume of about 1 mm in length and 0.1 mm in width. Further details of the laser system, accompanying instrumentation, and data processing techniques are provided by So *et al.*[19]

Because of the difference in refractive indexes of Plexiglas and air, the planes located at ± 17.8 mm away from the centerplane of the tube were actually inclined at 1° from the horizontal. The line along which velocities were measured for $y = 17.8$ mm therefore went from 17.3 mm above the centerplane at the internal wall surface at the outer bend radius to 18.3 mm on the internal wall surface at the inner bend radius. The uncertainty estimate for location was 1.5% in the measurement position on account of the finite length of the sampling volume and possible

Notation

a	Pipe radius = 3.81 cm
De	Dean number $\equiv \left(\frac{a}{R}\right)^{1/2}$ Re
g	Gravitational constant
Gr	Grashof number $\equiv \frac{g\beta(2a)^3(T_w - T_a)}{\nu^2}$
R	Radius of curvature of bend
Re	Reynolds number $\equiv \frac{W_{av}2a}{\nu}$
s	Axial distance along straight pipe; negative for upstream, positive for downstream
T_w	Pipe wall temperature
T_a	Air temperature inside pipe
U	Secondary or circumferential velocity
W	Axial velocity
W_{av}	Average velocity across pipe
y	Vertical distance measured from horizontal plane
α	Radius ratio $\equiv \frac{a}{R}$
β	Volumetric coefficient of thermal expansion
θ	Curve angle measured from bend entrance
ν	Kinematic viscosity of air at room temperature

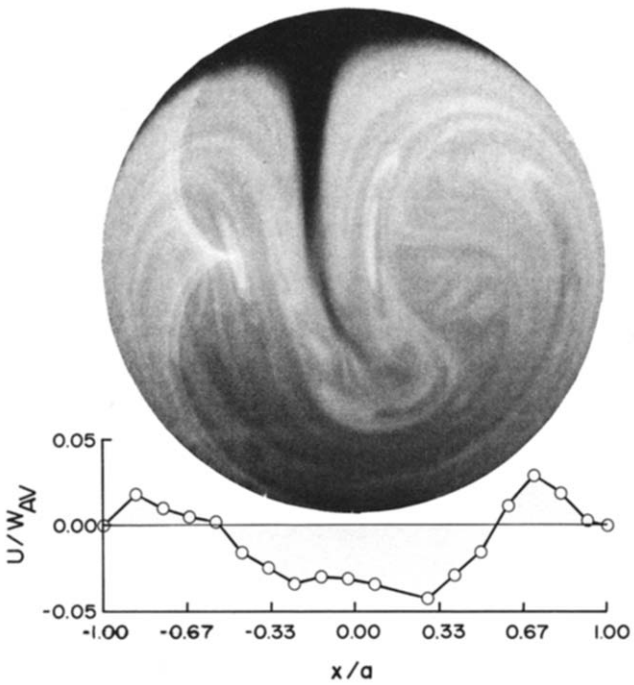

Figure 2 Buoyancy-induced secondary motion

nonuniformities in the pipe wall thickness. The uncertainty in the velocity data was 2.5% on account of possible variations in the flow rate over time and possible nonuniformities in the size of the seeding particles.

Qualification experiments

Preliminary measurements were made in the upstream pipe tangent outside the influence of the bend to demonstrate fully-developed laminar flow at Re≈400. However, these measurements did not yield a perfect parabolic velocity profile. To determine the cause of this variation, flow visualization was used to show qualitatively the flow characteristics. The flow was seeded with glycerine–water droplets, and a thin sheet of light was passed through the pipe perpendicular to its axis. Pictures were taken looking up the pipe, and a typical one obtained at 70 diameters downstream of the straight pipe entrance is shown in Figure 2. It presents clearly the secondary motion that occurs as a result of heat transfer between the pipe wall and the flow. The bright pattern in the left part of the picture was caused by the reflection of light off the left wall of the pipe. Figure 2 also shows a typical U velocity profile, measured in the horizontal plane of symmetry and normalized with respect to W_{av}, for the horizontal centerplane of the pipe. It shows a secondary motion—up near the wall of the pipe and down in the middle—resembling that shown in the accompanying picture.

Thermocouple measurements of the air and wall temperature show that the temperature difference between the pipe wall and air was 1°C or less, yielding Gr≈70,000. The Grashof number divided by the square of the Reynolds number is the ratio of the buoyancy force to the inertia force and gives a measure of the influence of buoyancy on the velocity distribution. In our study, this quantity amounted to about 0.44, showing that buoyancy effect was definitely important. To obtain a flow with negligible buoyancy effect, the temperature difference between the pipe wall and air would have to be 0.25°C or less, which is extremely difficult to attain without major modifications to the present rig. All attempts to eliminate the buoyancy effect in the flow within the present rig failed, including wrapping 25 mm thick pipe insulation along the entire length of the pipe. This shows one of the difficulties in establishing axisymmetric, fully developed, laminar pipe flow at low Reynolds numbers using air as the working fluid in the present rig. Very small temperature differences at low Re can create large Gr and a resulting variance from fully developed, axisymmetric laminar flow. If this effect is to be eliminated, an elaborate rig must be designed.

Since heat transfer effects distort the flow only in the vertical direction, and pipe curvature effects are evident only in the horizontal direction if the bend is oriented horizontally, the two effects can be separately identified in any profile measurements. Therefore, even with the difficulties associated with achieving fully developed isothermal, laminar air flow at low Re in the present rig, it was still possible to determine the influence of bend curvature on fully developed laminar flow by orienting the bend horizontally. A horizontal displacement of the velocity maximum indicates an effect of bend curvature, and a vertical displacement of the velocity maximum indicates buoyancy effects. In view of this, attempts to eliminate the buoyancy effects in the flow were abandoned, and later experiments were carried out with the buoyancy effects present.

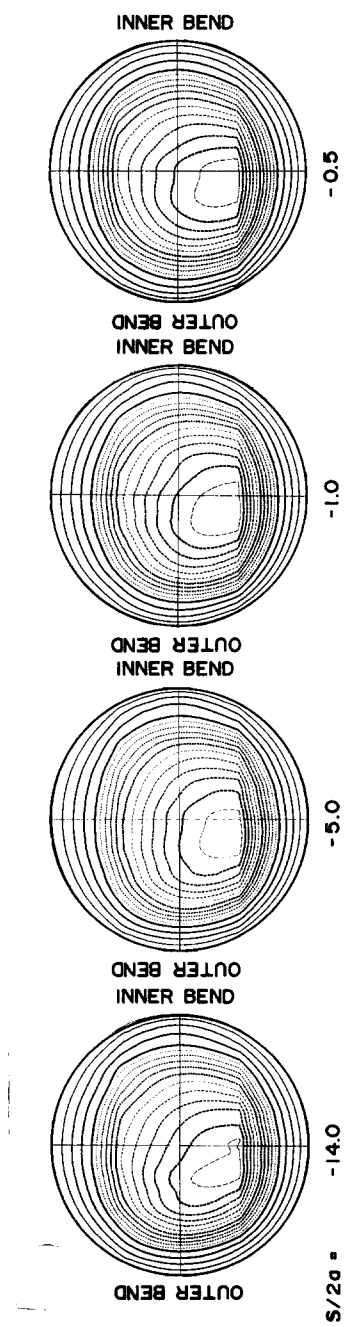

Figure 3 Axial velocity contours for flow leading up to bend—α=0.08 case

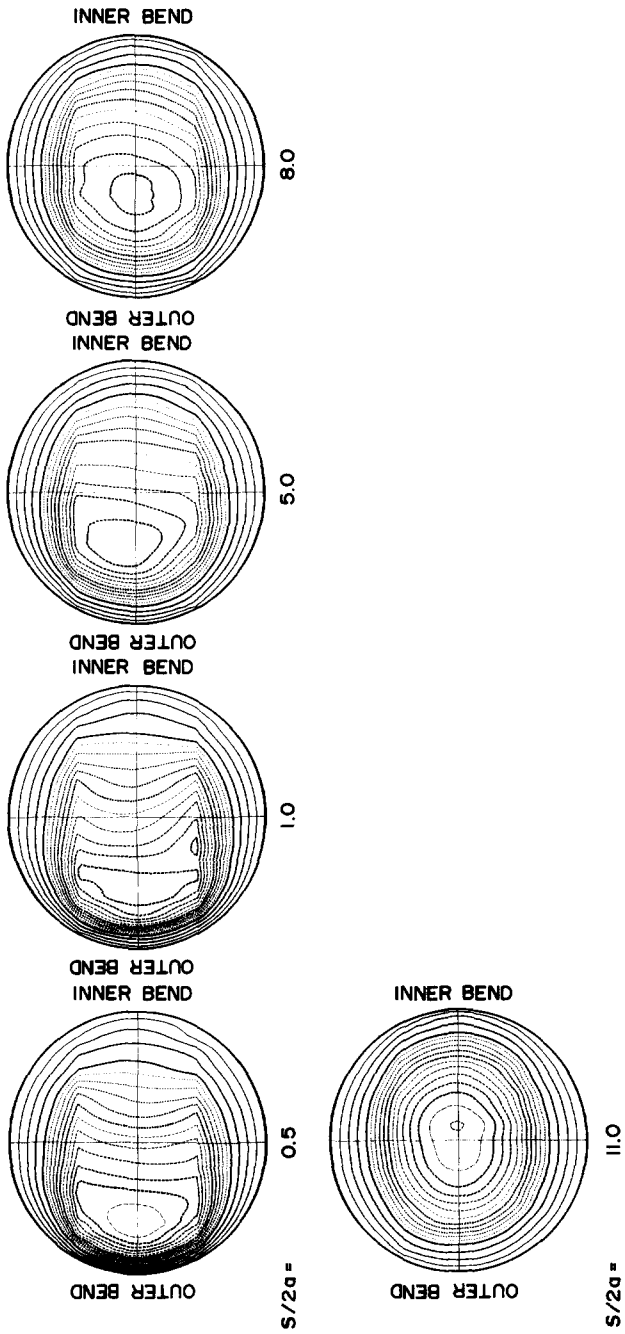

Figure 4 Axial velocity contours for flow downstream of bend—$\alpha=0.08$ case

Discussion of results

All experiments were carried out at a fixed Reynolds number, Re$\approx$ 400. This corresponds to a W_{av} value of about 8 cm/s. The two different bends investigated had radius ratios of about 0.08 and 0.30. Therefore, the corresponding De values are 110 and 220, respectively. Profile measurements at three different planes—$y/a=0$ and ± 0.46—were made at eight different stations upstream and nine different stations downstream of the bends. These stations are shown in Figure 1 in terms of the normalized distance $s/2a$. At the entrance to, and exit from, the bend, s was taken to be zero. These measurements were then used to construct isovelocity contours at each station after the velocity had been normalized by W_{av}. Cubic splines were used to fit the data points obtained from the three different measurement planes. Even though the number of data points available for constructing the contours is limited, the resulting contour plots still provide a good qualitative picture of the bend influence on the upstream and downstream flow. Isovelocity contour plots at selected stations for the $\alpha=0.08$ bend are shown in Figures 3 and 4, whereas those for the $\alpha=0.30$ bend are shown in Figures 5 and 6. Moreover, the velocity profiles at the symmetry plane ($y/a=0$) downstream of the bend for the two cases $\alpha=0.08$ and 0.3 are shown in Figures 7 and 8.

For flow through a pipe bend, a radial pressure gradient must exist across the pipe to balance the centrifugal force created by streamline curvature in the flow. The pressure is greatest near the outer wall (farthest from the center of curvature of the bend) and smallest near the inner wall. This, together with the fact that the fluid near the pipe wall moves slower than the fluid in the pipe center, helps to set up a secondary flow where the fluid in the middle of the pipe moves outward, impinges on the outer wall, and then turns to move inward along the top and bottom walls. As a result, the region of maximum velocity is displaced from the pipe center toward the outer wall. Although the

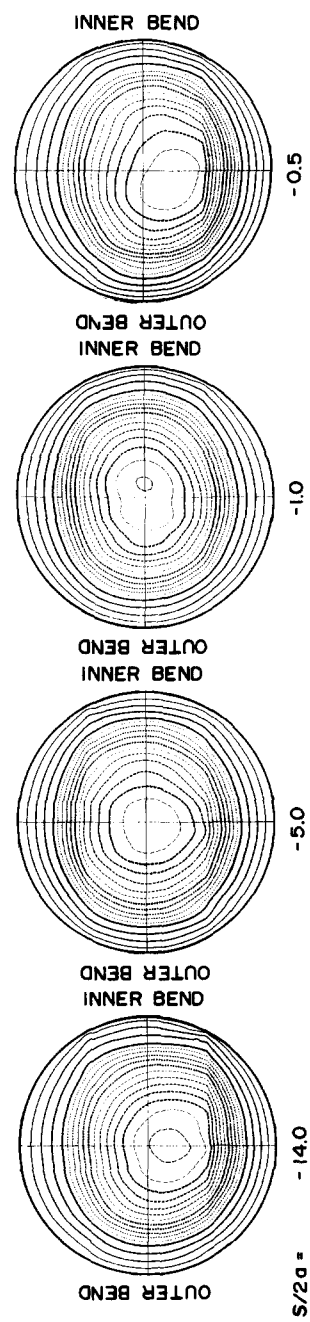

Figure 5 Axial velocity contours for flow leading up to bend $\alpha=0.3$ case

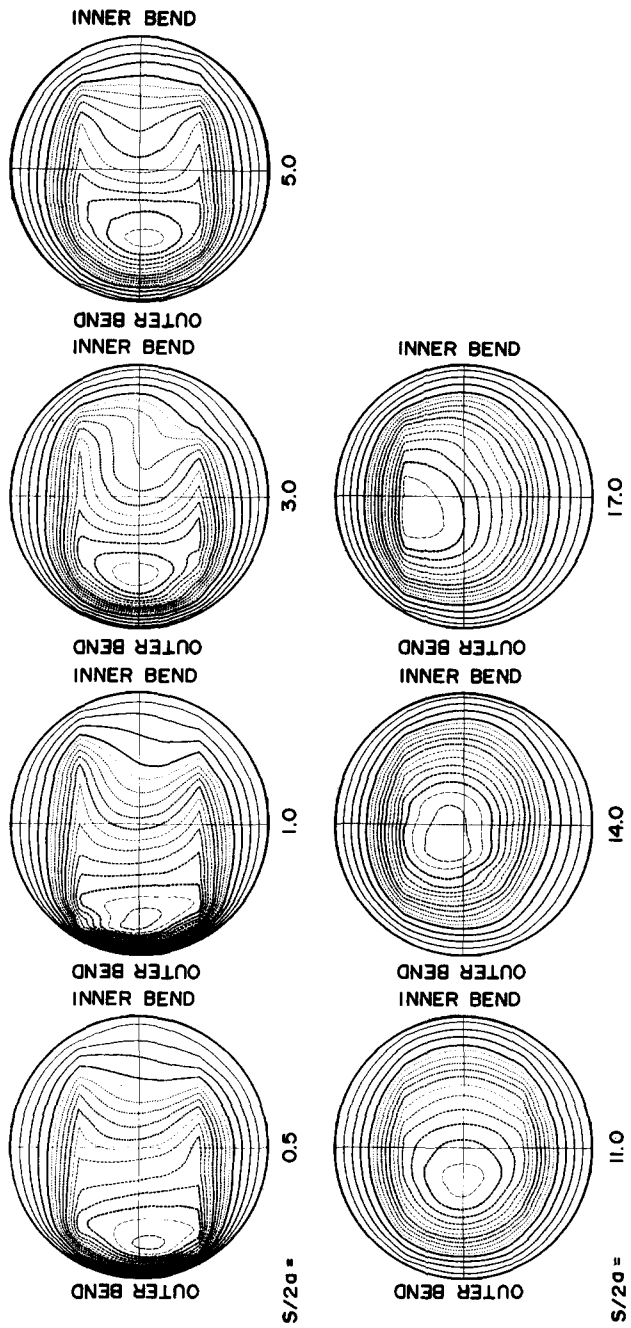

Figure 6 Axial velocity contours for flow downstream of bend—$\alpha=0.3$ case

centrifugal force is present only within the bend, the radial pressure gradient set up to balance it can propagate both upstream and downstream away from the bend. According to the analysis of Yao and So,[18] the pressure effect dies off exponentially and the resultant induced secondary motion in the upstream flow also vanishes exponentially. For $\alpha=0.30$, the analysis gives a U velocity equal to 2.5% of W_{av} at one-half diameter upstream, 1.1% at one diameter, and less than 0.2% at two diameters. When $\alpha=0.08$, even at one-half diameter upstream, the magnitude of U would be less than 1% of W_{av}. In view of this, a shift of the velocity maximum toward the outer wall should be detected at one-half diameter upstream for the $\alpha=0.30$ bend and none at all for the $\alpha=0.8$ bend. This is precisely what is observed in the measurements shown in Figures 3 and 5. The contour plots in Figure 5 show that the velocity maximum at one-half diameter has shifted toward the outer wall and is not symmetric about the horizontal pipe centerplane. Of course, the shift from the pipe centerplane toward the bottom wall is due to buoyancy effects and is noticed even at 5 and 14 diameters upstream. On the other hand, the contour plots at $s/2a=-0.5$, -1, -5, and -14 shown in Figure 3 for $\alpha=0.08$ are very similar and do not show the shift toward the outer wall other than the shift caused by buoyancy effects.

A shift of the velocity maximum toward the inner wall at one diameter upstream is noted in Figure 5 for the $\alpha=0.30$ bend.

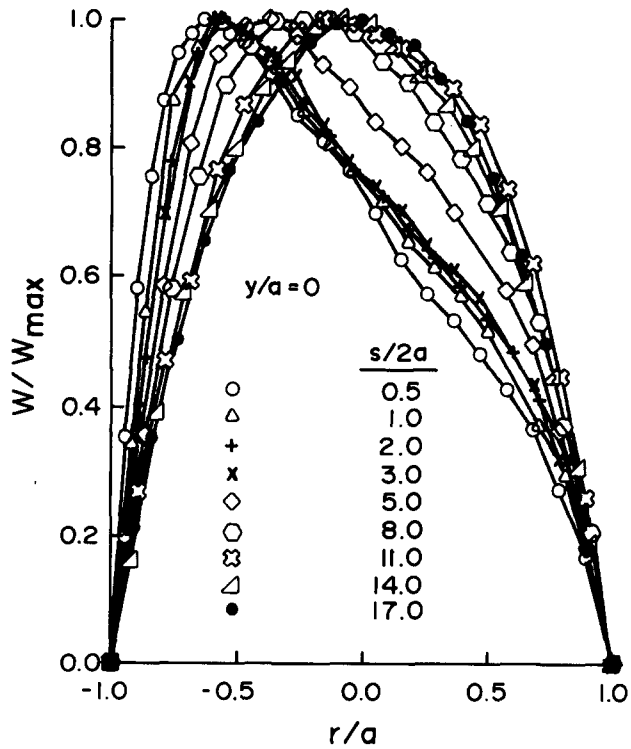

Figure 7 Profile plots of W/W_{max} in the plane of symmetry ($y/a=0$) downstream of the bend for $\alpha=0.08$

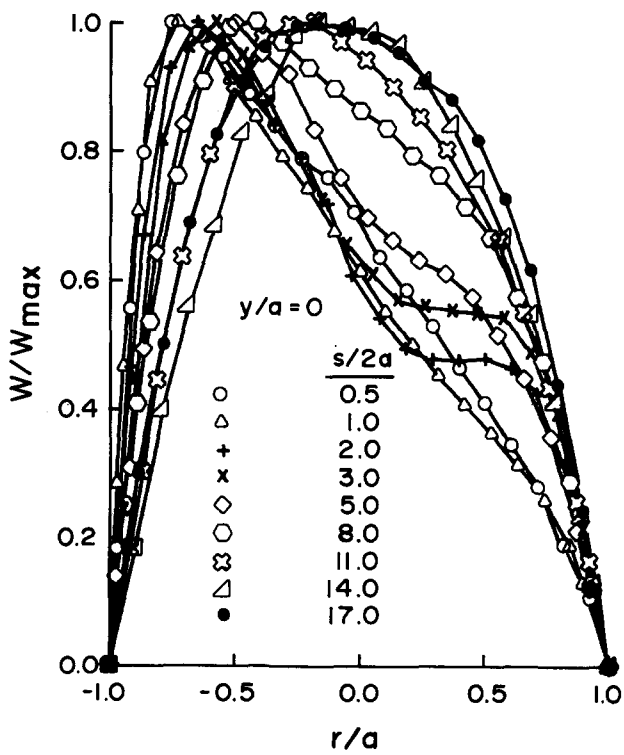

Figure 8 Profile plots of W/W_{max} in the plane of symmetry ($y/a=0$) downstream of the bend for $\alpha=0.30$

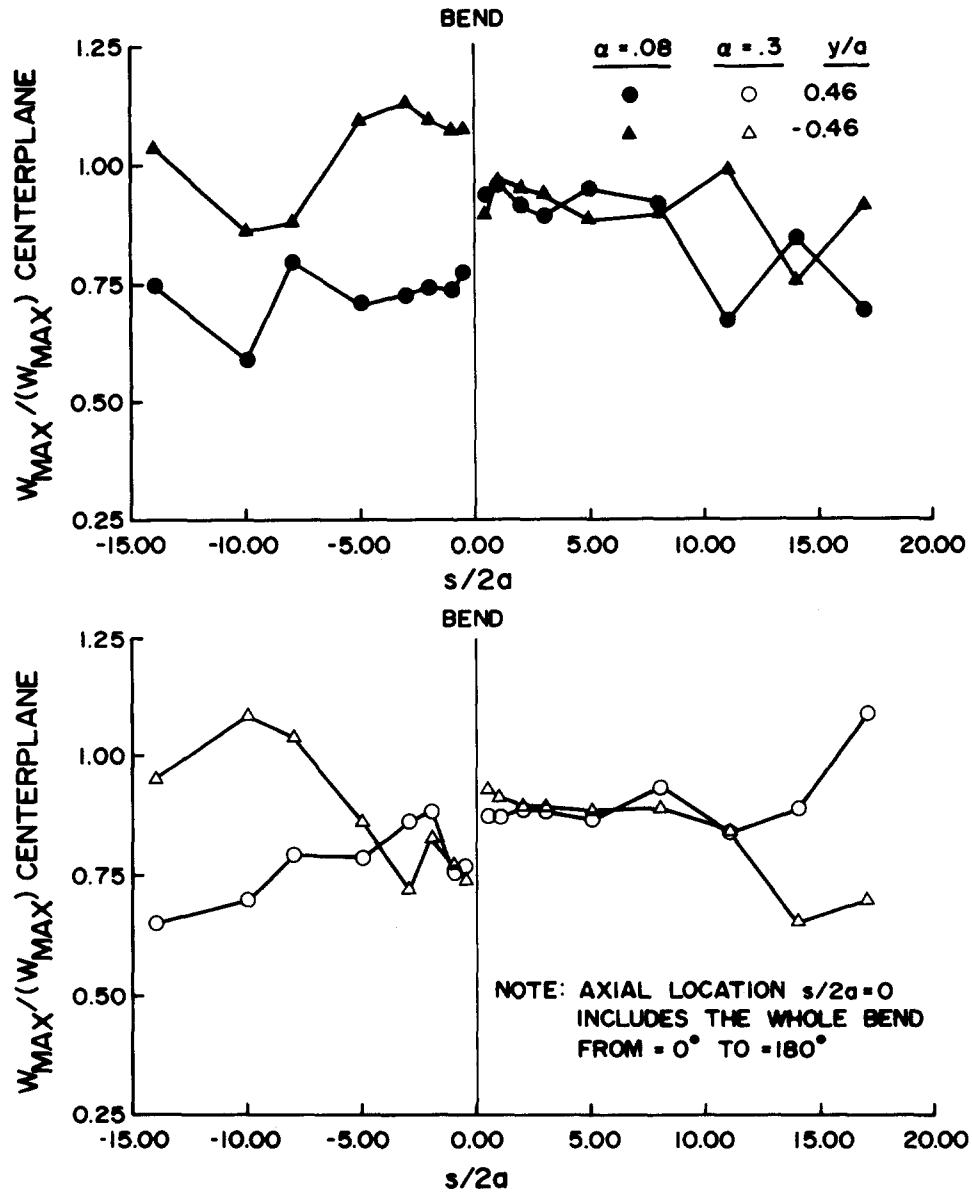

Figure 9 Effects of buoyancy on upstream and downstream flow through the bend

This could be explained by the fact that the flow in the straight pipe sees the bend as an obstruction at this location and speeds up to overcome the blockage. Similar results are also found in the study by Azzola and Humphrey.[6] They report a U velocity across the tube centerline, at two diameters upstream, of $<1.5\%$ of W_{av}. By one diameter upstream, this component increases to about 4% and is directed toward the inner wall. However, they have not measured the flow at one-half diameter. Therefore, the shift of the velocity maximum toward the outer wall in the tangent that connects to the curved pipe is not detected.

Coming out of the bend is a well-established secondary motion in the flow that will affect the flow recovery in addition to the pressure gradient effect set up by bend curvature. Even though the pressure gradient effect dies off exponentially according to Yao and So,[18] it will take a long distance to erase the secondary motion (or history effects) by viscous action. Therefore, downstram of the bend, one would expect the bend influence to last longer, and the recovery to fully developed laminar pipe flow would not be complete until many pipe diameters downstream. This is essentially shown in Figures 4 and 6. For the $\alpha=0.08$ bend, the recovery is complete at $s/2a=11$ (Figure 4), but it takes until $s/2a=14$ for the $\alpha=0.30$ bend to show fully developed flow characteristics again (Figure 6). Ito[15] measured the pressure drop along the downstream tangent of a turbulent flow coming out of a 90° bend with $\alpha=0.27$. He showed that the slope of the pressure drop curve approached the straight pipe slope asymptotically at 20 diameters downstream. Even though the present results are for laminar flows and $De\leqslant 220$, they are in qualitative agreement with Ito's measurements, which are for turbulent flow and $De\approx 10^5$.

The effect of bend curvature (or Dean number) is evident in these measurements. At one-half diameter downstream of the bend, the velocity maximum occurs at $0.76a$ for the $\alpha=0.30$ bend and at $0.63a$ for the $\alpha=0.08$ bend. Because of the stronger centrifugal force created by the tighter bend, the velocity maximum is forced farther from the tube center toward the outer wall for the $\alpha=0.30$ bend.

Another interesting feature in the downstream flow is observed in the $\alpha=0.3$ bend, where $De=220$. Figure 8 shows the development of a double-peak axial velocity profile at $s/2a=2$. This double peak remains visible until $s/2a=5$ and completely disappears at $s/2a=8$. However, such a behavior is not observed in the $\alpha=0.08$ bend (Figure 7). Similar characteristics are also reported by Agrawal *et al.*[9] and Olson and Snyder,[13] who report measurements within the bend only. In these studies, Agrawal *et al.*[9] measure a doubly peaked velocity profile like those shown in Figure 8 for $De=565$ but not for $De=183$, and Olson and Snyder[13] report the same behavior for $De=500$. Therefore, this

behavior seems to depend on Dean number and is not observed when $De < 200$.

The secondary motion induced by the bend has effectively damped out the buoyancy effects in the flow. The isovelocity contours at $s/2a \leqslant 8$ are observed to be approximately symmetrical about the horizontal pipe centerplane (Figures 4 and 6). A clear presentation of this observation is shown in Figure 9, where the maximum W values obtained from the off-center measurement planes for each axial location are plotted versus $s/2a$. These velocities are normalized by the local maximum centerplane velocity. If the velocity profile is truly parabolic, the values for the above- and below-centerplane maxima would be equivalent and equal to 0.78 at $y/a = \pm 0.46$. Therefore, Figure 9 shows the existence and development of the buoyancy effects on the flow as it moves through the bend. Immediately downstream of the bend ($s/2a < 8$), the difference between the two off-centerplane velocity maxima is very small compared with the large difference observed upstream and far downstream ($s/2a > 11$). This shows that the buoyancy effects have disappeared as a result of the strong mixing created by the curvature-induced secondary current within the bend. As this secondary current slowly disappears downstream, the secondary motion created by buoyancy effects become dominant again, thus giving rise to the observed difference between the two off-centerplane velocity maxima.

Conclusions

Failure to establish a fully developed axisymmetric laminar flow through the straight pipe in the present simple rig shows the difficulty in achieving such flow condition at low Reynolds number using air as the working fluid. For an Re value of 400, a temperature difference of only 1°C between the pipe wall and air yields $Gr \approx 70{,}000$. The Grashof number divided by Re^2 is a measure of the ratio of the buoyancy force to the inertia force. For our study, this quantity amounted to about 0.44. Therefore, buoyancy effects were important in this flow.

Despite this, it is still possible to ascertain the extent of the influence of the bend on the upstream and downstream flow provided the bend is oriented horizontally. For flow with $De = 110$, no upstream influence on the axial velocity was detected. When De was increased to 220, the maximum axial velocity was observed to shift toward the inner wall at about one diameter upstream and then toward the outer wall at $s/2a = -0.5$. Recovery from bend curvature effect took longer downstream. This was due to the slow viscous action on the flow. For the $\alpha = 0.30$ bend ($De = 220$), recovery was complete at $s/2a = 14$, but for the $\alpha = 0.08$ bend ($De = 110$), it took only 11 diameters to achieve complete recovery. The measured flow characteristics are consistent with those observed by other researchers. In particular, the measured upstream influence is in good qualitative agreement with the analysis of Yao and So.[18]

Acknowledgement

Research support by ONR Grant No. N0014-81-K-0428 is gratefully acknowledged.

References

1 Dean, W. R. Note on the motion of fluid in a curved pipe. *Phil. Mag.*, 1927, **20**, 208–223.
2 Dean, W. R. The streamline motion of fluid in a curved pipe. *Phil Mag.*, 1928, **30**, 673–693.
3 Berger, S. A., Talbot, L., and Yao, L. S. Flow in curved pipes. *Ann. Rev. Fluid Mech.*, 1983, **15**, 461–512.
4 Yao, L. S., and Berger, S. A. Entry flow in a curved pipe. *J. Fluid Mech.*, 1975, **67**, 177–196.
5 Prusa, J., and Yao, L. S. Numerical solution for fully-developed flow in heated curved tubes. *J. Fluid Mech.*, 1982, **123**, 503–522.
6 Azzola, J., and Humphrey, J. A. C. Developing turbulent flow in a 180° curved pipe and its downstream tangent. Paper presented at the Second International Symposium on Applications of Laser Anemometry to Fluid Mechanics, 2–4 July, 1984, Lisbon, Portugal.
7 Patankar, S. V., Pratap, V. S., and Spalding, D. B. Prediction of turbulent flow in curved pipes. *J. Fluid Mech.*, 1975, **57**, 583–595.
8 Wang, C. Y. On the low Reynolds number flow in a helical pipe. *J. Fluid Mech.*, 1981, **108**, 185–194.
9 Agrawal, Y., Talbot, L., and Gong, K. Laser anemometer study of flow developed in curved circular pipes. *J. Fluid Mech.*, 1978, **85**, 497–518.
10 Humphrey, J. A. C., Iacovides, H., and Launder, B. E. Some numerical experiments on developing flow in circular-sectioned bends. *J. Fluid Mech.*, 1985, **154**, 357–375.
11 Hille, P., Vehrenkamp, R., and Schulz-Dubois, E. O. The development and structure of primary and secondary flow in a curve square duct. *J. Fluid Mech.*, 1985, **141**, 219–241.
12 Taylor, A. M. K. P., Whitelaw, J. H., and Yianneskis, M. *Measurements of laminar and turbulent flow in a curved duct with thin inlet boundary layers.* NASA CR-3367, 1981.
13 Olson, D. E., and Snyder, B. The upstream scale of flow development in curved circular pipes. *J. Fluid Mech.*, 1985, **150**, 139–158.
14 Sreenivasan, K. R., and Strykowski, P. J. Stabilization effects in flow through helically coiled pipes. *Exp. in Fluids*, 1983, **1**, 31–36.
15 Ito, H. Pressure loss in smooth pipe bends. *J. Basic Eng.*, 1960, **82**, 131–143.
16 Rowe, M. Measurements and computations of flow in pipe bends. *J. Fluid Mech.*, 1970, **43**, 771–783.
17 Enayet, M. M., Gibson, M. M., Taylor, A. M. K. P., and Yianneskis, M. Laser-Doppler measurements of laminar and turbulent flow in a pipe bend. *Int. J. Heat and Fluid Flow*, 1982, **3**, 213–219.
18 Yao, L. S., and So, R. M. C. Asymptotic analysis of turbulence structure in the entry region of a curved pipe. Submitted to *J. Fluid Mech.*, 1986.
19 So, R. M. C., Ahmed, S. A., and Mongia, H. C. *An experimental investigation of gas jets in confined swirling air flow.* NASA CR-3832, 1984; also, *Exp. in Fluids*, 1985, **3**, 221–230.